Chemical Methodologies

Journal homepage: http://chemmethod.com

*Original Research Article*

# Radiation Hazards Investigation of Photon Scattering by Elekta 6 MeV Linac during Liver Cancer Treatment

**Neda Zarei[1], Mohammad Reza Rezaie[1,*], Ali Jomehzadeh[2]**

[1]*Department of Nuclear Engineering, Faculty of Sciences and Modern Technologies, Graduate University of Advanced Technology, Kerman, Iran*

[2]*Medical physics Department, Medical School, Kerman University of Medical Sciences, Kerman, Iran*

**ARTICLE INFO**

**Article history**

Submitted: 2022-03-23

Revised: 2022-04-12

Accepted: 2022-05-18

Manuscript ID: CHEMM-2204-1493

Checked for Plagiarism: **Yes**

Language Editor:

Dr. Behrouz Jamalvandi

Editor who approved publication:

Professor Dr. Hassan Karimi-Maleh

**DOI**:10.22034/CHEMM.2022.338957.1493

**KEYWORDS**

Elekta accelerator
Photon scattering
MIRD phantom
MCNPX
GEANT4
Radiation hazards
Dose

**ABSTRACT**

Medical accelerators such as Elekta linac are used to treat cancer and imaging. Depending on cancer type, they regulate certain field size. Because of photon scattering from accelerator components, for every field size to treat cancer, air and patient's body, there is the radiation risk for other organs. In this research, the scattering factor for different fields of Elekta linac is first calculated using the phase space specifications in GEANT4 and MCNPX codes. Due to the scattering of photons, the calculated dose in other body organs in the treatment of liver cancer was calculated using the MIRD phantom and the accelerator phase space. For 15 Gy dose in liver cancer treatment, the other organs also receive a significant dose due to their distance from the liver. Even brain tissue that is far from the liver and is out of treatment plan receives about 0.47 Gy dose. One of the major problems of radiotherapy is the inability to accurately focus on the radiation field size of the cancerous tissue. Even by precisely adjusting the field size to the tumor size, there is a risk of radiation to the tissues around the tumor due to the scattering of photons from the air, accelerator components, and patients' body parts. Until now, it has been assumed that small volumes of healthy tissue around the tumor are at radiation risk in radiotherapy procedures. However, the results of this study showed that the radiation risk from radiotherapy procedures is much higher in the tissues near the tumor.

**GRAPHICAL ABSTRACT**

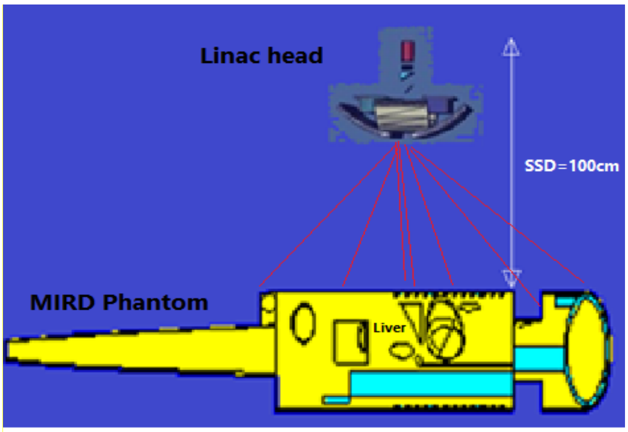


* Corresponding author: Mohammad Reza Rezaie

✉ E-mail: mr.rezaie@kgut.ac.ir

## Introduction

Radiation therapy is a treatment that plays a key role in the fight against cancer [1]. This radiation can be applied from outside the patient's body (remote treatment) or by placing radioactive materials in the patient's body (brachytherapy). In remote therapy, linear medical accelerators are used to obtain photons or electrons energy in the MeV range, as well as proton beams and heavy ions. Photons in this energy range allow the treatment of tumors in the body. The radiation fields are formed by a collimator system on the linear accelerator (linac) head, creating fields that are formed separately for the target treatment volume. The accelerator head is mounted in such a way that it can rotate around the patient at any desired angle. In this way, the rays can be irradiated from different directions, thus maintaining healthy tissue and important organs and focusing on the tumor tissue [2]. Previous research has shown that Monte Carlo methods are suitable for simulating photon beam transport in linear medical accelerators. Simulation methods can be used to measure the dose distribution in phantoms and patients' body. Geant4 toolkit [3] and MCNPX code were used to determine the phase space specification of the 6 MeV Elekta compact accelerator. MCNPX code based on the Monte Carlo method is capable of transporting 32 atomic particles and nuclei in different environments [4]. Geometry and Tracking toolkit (Geant4) is a simulation software based on the Monte Carlo method that written in C++ software and tracks all kinds of particles and has the ability to simulate magnetic and gravity fields and photon transport in nanoscale. Geant4 has many libraries with different particle cross sections in different environments [5]. In this method, the spatial, angular, and energy spectra of X-ray colliding with the tungsten target are extracted and its information is introduced as phase space. The spectral information of the phase space is defined as the X-ray source in the Geant4 toolkit and MCNPX code of the Elekta Compact accelerator for calculation of total scattering coefficient (Scp). Scp is not calculated for the compact model Elekta accelerator till now. Scattering factor calculations show the scattering of photons from the accelerator components and the patient's body. Therefore, it is possible for the out-of-field dose to reach other parts of the body in the treatment of cancer in a particular organ. To examine out-of-field dose, a Medical Internal Radiation Dose (MIRD) phantom [6] is defined on the patient's bed in treatment room under the Elekta linac head, and by defining the space phase as a source above the target, the possibility of out-of-field doses in other organs of the body in the treatment of liver cancer using the MCNPX code is examined. The method is described in the section below.

## Materials and Methods

The research was done in three steps. First, the phase space of the Elekta linac was calculated using the Geant4 toolkit and MCNPX code. Then, the scattering factor was calculated using the accelerator phase space. Finally, dose evaluation was performed inside MIRD phantom for the treatment of liver cancer, the out-of-field dose in other organs was also calculated. Each of these steps is explained below.

### *Calculating phase space and scattering factor*

Geant4 Toolkit and MCNPX code were used to extract the Elekta compact linear accelerator phase space and calculations related to the total scattering factor (Scp). To extract data related to phase space and Scp, the geometry of the Elekta 6 MeV accelerator head was defined according to Figure 1, in which the accelerator head is composed of the following parts: a) Target: A tungsten cylinder with a radius of 2 mm b) Primary colimator: A tungsten cylinder with 10.2 cm high with a Frustum of a Cone. c) Flattening filter: tungsten cone with a height of 1.75 cm, d) Ionization chamber: thin cylindrical layers of copper, plastic and air with a total thickness of 1.5 cm and a radius of 3 cm [7]. e) Mirror: A Capton cylinder with 45-degree. f) Jaws x and y: tungsten cylindrical shells to adjust the field, and finally g) water phantom with the RK304 detector that is located at 10 cm from the water surface.

To perform the simulation, the electron spectrum of the accelerator source was required. The electron source has a Gaussian distribution with an average energy of 6 MeV and a width at half height equal to 3% of the average energy or standard deviation of 0.07 [8-11].

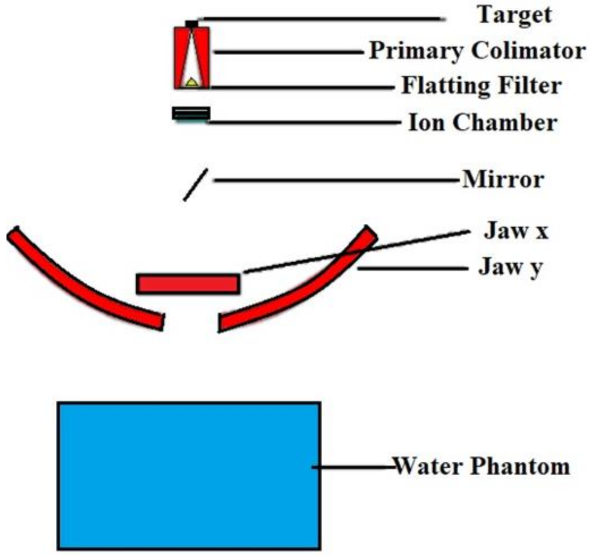


**Figure 1:** Head geometry of the compact elekta linear accelerator

An input file was required to run the simulation program. Geometry information and accelerator source were written in the necessary files for simulation by GEANT4 Toolkit and MCNPX code data and prepared for computer execution. The simulation was performed using a 7-core computer with 8 GB of RAM and a 2.9 GHz CPU. By running the code and stopping the electron in target, an X-ray is generated. The X-ray spectrum changes through different parts of accelerator head due to the absorption of photons and the production of secondary photons due to the interaction of photons with matter [12], and its intensity decreases and the spectrum becomes weaker at low energies. X-rays are produced at a 0-0.2 MeV range, which is considered as a photon source. In order to perform dosimetry calculations with high accuracy, the program must be run for several days. To solve this problem, the accelerator phase space must be calculated and defined in GEANT4 Toolkit and MCNPX code files. Phase space contains spatial information [13], energy and angles of the secondary photons passed over target in the accelerator head, which is obtained by running the GEANT4 Toolkit and MCNPX code. After calculating the phase space and by defining the phase space data in the GEANT4 Toolkit and MCNPX code, the Scp at a depth of 10 cm of water phantom for 5×5, 10×10, 20×20, 25×25 and 30×30 $cm^2$ field sizes were calculated. Scp is equal to the dose ratio at a depth of 10 cm for each field size to a dose at a depth of 10 cm of the reference field 10 × 10 $cm^2$ [14].

*Cancer risk (ELCR) and Out-of-field dose calculations in liver cancer radiotherapy*

Lifetime cancer risk is calculated by quantifying the risk of cancer (ELCR) using Equation 1 [15].

$$ELCR = D \times RF \qquad (1)$$

In Equation 1 D(Sv) is the out-of-field dose and RF Risk factor ($Sv^{-1}$) indicates the risk of fatal cancer in each organ. For random effects, this value is 0.05 according to ICRP 60 [16-17].

To calculate the out-of-field dose in liver cancer radiotherapy, a MIRD phantom is placed on a patient bed 100 cm below the accelerator head as shown in Figure 2. The phase space is defined as a source above the target. By adjusting the patient bed and field size, the accelerator prepares to irradiate the liver tissue in the MIRD phantom. By executing the code, the amount of dose received in the liver tissue and other organs of the body is calculated in unit of MeV/g per source particle using f6 tally. The following coefficients are considered to convert the f6 tally output to Gy.

1. The probability of producing a photon due to the collision of an electron that is 0.86.
2. The conversion factor of MeV/g to Gy that is 1.6e10.
3. Coefficient of accelerator current

Relationship between accelerator current I(mA), number of electrons (n) and irradiation time t(s) is (I=ne/t). The number of electrons is n = It / e. For t=1 s and I=4 mA, the number of electrons is

$$4e\text{-}3 \times 1/1.6e\text{-}19 = 2.5e16$$

4. Coefficient related to irradiation time

Previous coefficients are calculated for the irradiation time as 1 second. If the irradiation time is t seconds, the result must be multiplied by the irradiation time to calculate the dose.

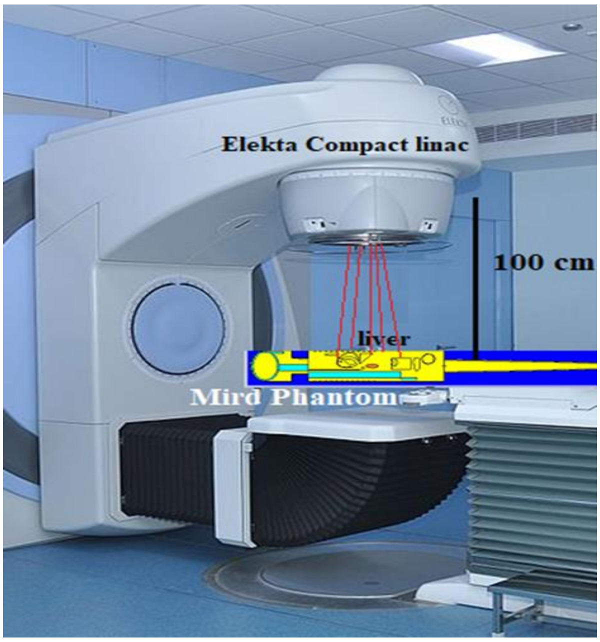


**Figure 2:** MIRD phantom under the head of the compact model Electra accelerator

## Results and Discussion

*The results of phase space calculation*

By placing a detector cell in different parts of the accelerator head, the characteristics of energy spectrum, angular distribution and spatial distribution of generated and passed photons were calculated. The energy spectrum and angular distribution of the photons produced after the target and the spatial distribution of the photons passed after the flattening filter are shown in Figures 3, 4 and 5.

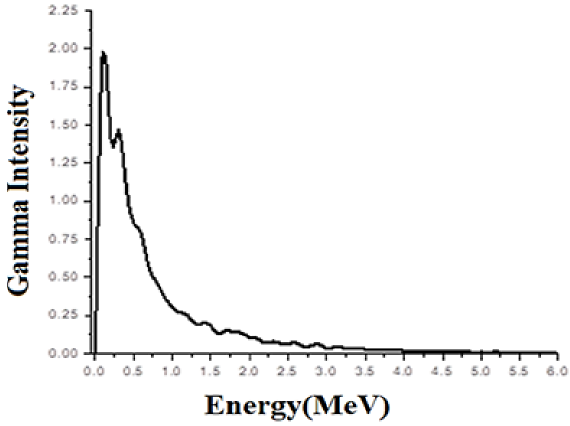


**Figure 3:** X-ray spectrum produced in the Compact Elekta accelerator

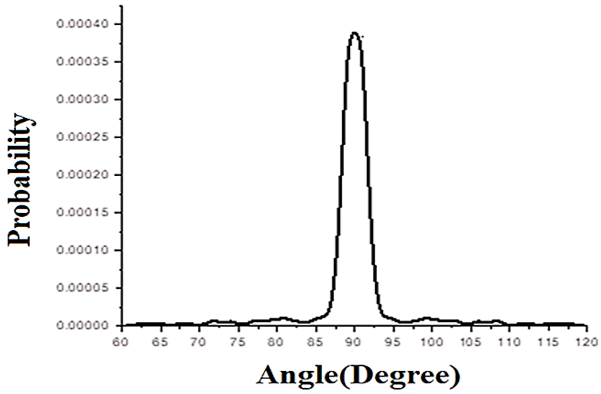


**Figure 4:** Angular distribution of X-rays generated in the head of the Compact model accelerator

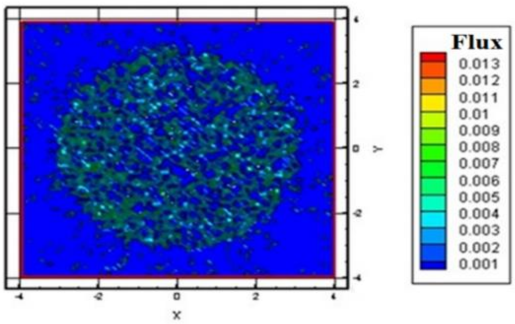


**Figure 5:** Spatial distribution of photons on a plane perpendicular to the accelerator axis after flattening filter

According to Figure 4, the angular distribution of the X-rays produced is a Gaussian distribution with standard deviation of 1.33 degrees and a half-height width of 3.12 degrees. According to Figure 5, the spatial distribution of photons emitted from the target in different parts of the accelerator shows that the spatial distribution has a uniform distribution perpendicular to the axis of the accelerator.

Therefore, three characteristics of the energy spectrum, angular distribution and spatial distribution in Figures 3, 4 and 5 can be considered as the phase space characteristics of photons produced by the collision of an electron beam with a target.

*Results of scattering factor calculation*

By defining the phase space data in the GEANT4 Toolkit and MCNPX code, the Scp at a depth of 10 cm of water phantom for 5 × 5, 10 × 10, 20 × 20, 25 × 25 and 30 × 30 $cm^2$ field sizes was calculated. The result was shown that with increasing the field size, the Scp increased, due to the scattering of photons by Jaws and other accelerator components. The results of the Scp calculation by GEANT4 Toolkit and MCNPX code are given in Table 1. Table 2 shows the percentage agreement between experimental and theoretical calculation of Scp by GEANT4 Toolkit and MCNPX code. The results in Table 2 show that there is a 96% and 93% agreement between the MCNPX and GEANT4 simulations, and practical values of Scp, respectively.

**Table 1:** Results of Experimental and theoretical calculation of Scp by GEANT4 Toolkit and MCNPX code

| Experimental data | | | Using phase space | | |
|---|---|---|---|---|---|
| 18 | 11 | 10 | MCNPX | GEANT4 | Field size ($cm^2$) |
| 0.80 | 0.95 | 0.90 | 0.82 | 0.98 | 5×5 |
| 1.00 | 0.98 | 1.00 | 1.00 | 1.00 | 10×10 |
| 1.18 | 1.10 | 1.19 | 1.13 | 1.21 | 20×20 |
| 1.19 | 1.12 | 1.10 | 1.15 | 1.23 | 25×25 |
| 1.20 | 1.15 | 1.12 | 1.18 | 1.25 | 30×30 |

**Table 2:** The Compatibility level between practical and MCNPX and GEANT4 simulation value of Scp

| GEANT4 93% | | | MCNPX 96% | | |
|---|---|---|---|---|---|
| 18 | 11 | 10 | 18 | 11 | 10 |
| 0.911111 | 0.968421 | 0.775 | 0.911111 | 0.863158 | 0.975 |
| 1 | 0.979592 | 1 | 1 | 0.979592 | 1 |
| 0.983193 | 0.9 | 0.974576 | 0.94958 | 0.972727 | 0.957627 |
| 0.881818 | 0.901786 | 0.966387 | 0.954545 | 0.973214 | 0.966387 |
| 0.883929 | 0.913043 | 0.958333 | 0.946429 | 0.973913 | 0.983333 |

*Results of out-of-field dose calculation*

By applying the phase space characteristics above target in the head of the Elekta accelerator and by adjusting the field as 25×25, 20×20, 10×10, 5×5 and 30 × 30 $cm^2$, the out-of-field dose calculation for liver cancer treatment was examined. The results show that the reached dose is significantly outside the above fields due to the scattering of photons. The 5×5 $cm^2$ field size was found to be suitable for irradiation to the liver organ.

As can be seen from Figure 6, the dose reaches outside the 5×5 $cm^2$ field size, which indicates the scattering of X-ray photons by the accelerator components, the environment and the patient's body. The dose reached the liver and other organs were also calculated using the f6 tally if a 45 Gy dose was injected into the liver to treat cancer. Table 3 shows the results of the dose reached other organs in the treatment of liver cancer with a dose of 45 Gy.

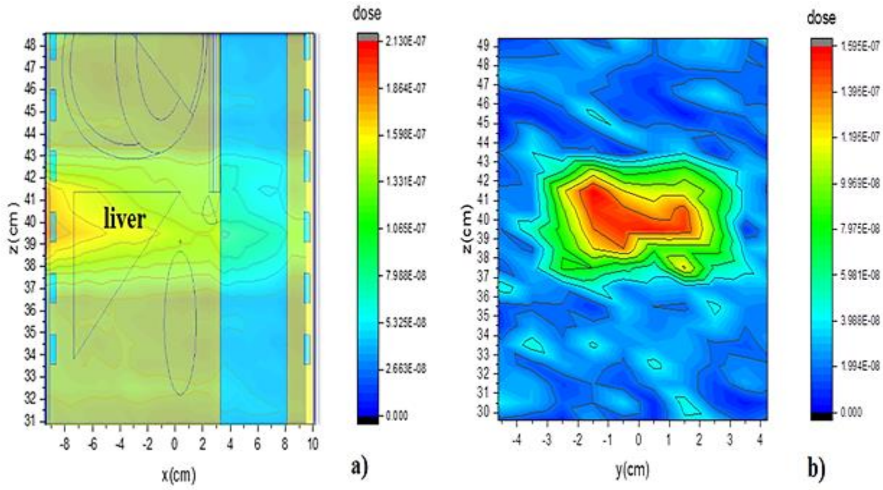


**Figure 6:** Dose distribution around the liver for 5 ×5 cm$^2$ field size: a) depth dose distribution, b) surface dose distribution

**Table 3:** The dose reached to other organs in the treatment of liver cancer with a dose of 45 Gy

| Organ | Dose (Gy) | equivalent dose (Sv/Gy) | ELCR (%) |
|---|---|---|---|
| pancreas | 31.5163 | 2.101087 | 1.575815 |
| liver | 14.9906 | 0.999373 | 0.74953 |
| esophagus | 14.14383 | 0.942922 | 0.707192 |
| spine | 9.83569 | 0.655713 | 0.491785 |
| adrenals | 7.43699 | 0.495799 | 0.37185 |
| rib cage | 4.52829 | 0.301886 | 0.226415 |
| heart | 3.65228 | 0.243485 | 0.182614 |
| stomach | 3.03892 | 0.202595 | 0.151946 |
| kidneys | 2.56241 | 0.170827 | 0.128121 |
| Other | 2.47911 | 0.165274 | 0.123956 |
| lungs | 2.42233 | 0.161489 | 0.121117 |
| bladder and content | 2.02266 | 0.134844 | 0.101133 |
| spleen | 1.97659 | 0.131773 | 0.09883 |
| gall bladder | 1.93902 | 0.129268 | 0.096951 |
| skin | 1.80132 | 0.120088 | 0.090066 |
| small intestine | 1.669502 | 0.1113 | 0.083475 |
| colon and contens | 1.664198 | 0.110947 | 0.08321 |
| arm bones | 1.641877 | 0.109458 | 0.082094 |
| testes | 1.635961 | 0.109064 | 0.081798 |
| thymus | 1.62044 | 0.108029 | 0.081022 |
| pelvis | 1.447193 | 0.09648 | 0.07236 |
| thyroid | 1.322957 | 0.088197 | 0.066148 |
| male genitalia | 1.222589 | 0.081506 | 0.061129 |
| facial skeleton | 1.118532 | 0.074569 | 0.055927 |
| clavicles | 0.964971 | 0.064331 | 0.048249 |
| leg bones | 0.720749 | 0.04805 | 0.036037 |
| skull | 0.597499 | 0.039833 | 0.029875 |
| brain | 0.470798 | 0.031387 | 0.02354 |

Other= over skeleton; leg bones, arm bone, scapulae, pelvis, rib cage, spine, skull-cranium, facial skeleton

## Conclusion

Accelerators are widely used to treat cancer. Compact model Elekta accelerator is one of the types of linear accelerators in Iran that is used for this purpose. Usually, a treatment plan adjusted to the size of tumors in the target tissue is planned for the treatment of cancer. The goal is to deliver the highest dose to the target tissue and the lowest dose to the adjacent tissues. However, due to the scattering of X-ray photons from different parts of the accelerator, the environment and the patient's body tissues adjacent to the target tissue are also at risk. In this paper, we first calculated the scattering factor of photons in different fields. By calculating the scattering factor, the results showed that Scp increases with increasing field size. To calculate the scattering factor, the accelerator phase space data with Geant4 Toolkit and MCNPX code were used. Phase space was used to speed up the calculations. Then, the characteristics of the phase space were assumed as a photon source at the target location of the accelerator head. The case designed for the treatment of 15Gy liver cancer was calculated. The results showed that the pancreas receives a dose greater than 15 Gy due to its proximity to the target tissue and the organs around the liver receive a dose less than 15 due to their distance from the liver. The effect of air on photon scattering and increasing dose and dose leakage was calculated to be 6.69% . This study was devoted to determining the unwanted dose due to scattered photons to the out-of-field organs and subsequently estimated the risk of secondary cancers in the patients undergoing liver radiotherapy. A Medical Linear Accelerator (Compact Elekta 6 MV) was modeled using the Geant4 Toolkit and MCNPX code to simulate liver radiotherapy with different field size. Dose evaluation was performed inside MIRD phantom. The average photon equivalent dose in out-of-field organs is between 2.1-0.031 Sv $Gy^{-1}$, for the organs far from the Planning Treatment Volume (Brain) and those close to the treatment field (pancreas). Evidence showed that pancreas with 1.58% and Brain with 0.024% have the highest and lowest risk of secondary cancer, respectively. Accordingly, this study introduced the pancreas as an organ with a high risk of secondary cancer which should be paid more attention in the follow-up of patients undergoing liver radiotherapy. The results of this study showed that radiologists should be more careful in their treatment plan because of the possibility of secondary cancer in the tissues far from the field size.

## Acknowledgments

The authors would like to thank all technicians of Shafa Hospital Nuclear Medical Center for providing us technical support required for carrying out this work.

## Funding

This research did not receive any specific grant from funding agencies in the public, commercial, or not-for-profit sectors.

## Authors' contributions

Neda Zarei and Dr. Mohammad Reza Rezaie designed and simulated this study and Dr. Ali Jomehzadeh analyzed the data. Neda Zarei proceeded to the data quality control and the manuscript drafting. Mohammad Reza Rezaie revised the final version.

## Conflict of Interest

None of the authors has any conflict of interest to declare.

## ORCID:

*Neda Zarei*
*https://www.orcid.org/0000-0003-2090-5926*
*Mohammad Reza Rezaie*
*https://www.orcid.org/0000-0002-2183-7729*
*Ali Jomehzadeh*
*https://www.orcid.org/0000-0002-6729-2891*

## References

[1]. Abshire D., Lang M.K., The evolution of radiation therapy in treating cancer, *Seminars in oncology nursing*, 2018, **34**:151 [Crossref], [Google Scholar], [Publisher]

[2]. Falk S., Principles of cancer treatment by radiotherapy, *Surgery (Oxford)*, 2006, **24**:62 [Crossref], [Google Scholar], [Publisher]

[3]. Archambault L., Beaulieu L., Carrier J.F., Castrovillari F., Chauvie S., Foppiano F., Ghiso G., Guatelli S., Incerti S.E., Lamanna E., Larsson S., Overview of Geant4 applications in medical physics, In *2003 IEEE Nuclear Science Symposium. Conference Record (IEEE Cat. No. 03CH37515)*, 2003, **3**:1743, IEEE. [Crossref], [Google Scholar], [Publisher]

[4]. Hendricks J.S., *MCNPX version 2.5. c* (No. LA-UR-03-2202). Los Alamos National Lab.(LANL), Los Alamos, NM (United States), 2003 [Google Scholar]

[5]. Agostinelli S., Allison J., Amako K.A., Apostolakis J., Araujo H., Arce P., Asai M., Axen D., Banerjee S., Barrand G.J.N.I., Behner F., GEANT4—a simulation toolkit, *Nuclear instruments and methods in physics research section A: Accelerators, Spectrometers, Detectors and Associated Equipment*, 2003, **506**:250 [Crossref], [Google Scholar], [Publisher]

[6]. Geraily G., Elmtalab S., Mohammadi N., Alirezaei Z., Martinez-Ovalle S., Jabbari I., Vega-Carrillo H.R., Karimi A.H., Monte Carlo evaluation of out-of-field dose in 18 MV pelvic radiotherapy using a simplified female MIRD phantom, *Biomedical Physics & Engineering Express*, 2021, **8**:015004 [Google Scholar], [Publisher]

[7]. Krim D.E., Rrhioua A., Zerfaoui M., Bakari D., Oulhouq Y., Bouta M., Simulation of the patient-dependent part 6 MV Elekta linac photon beam using GATE, In *2019 International Conference on Intelligent Systems and Advanced Computing Sciences (ISACS)*, 2019, 1, IEEE [Crossref], [Google Scholar], [Publisher]

[8]. Sadoughi H.R., Nasseri S., Momennezhad M., Sadeghi H.R., Bahreyni-Toosi M.H., A comparison between GATE and MCNPX Monte Carlo codes in simulation of medical linear accelerator, *Journal of medical signals and sensors,* 2014, **4**:10 [Crossref], [Google Scholar], [Publisher]

[9]. McLaughlin D., Energy spectra comparisons for matched clinical electron beams on Elekta linear accelerators using a permanent magnet spectrometer. LSU Master's Theses. 2013 [Google Scholar], [Publisher]

[10]. Jelen U., Dong B., Begg J., Roberts N., Whelan B., Keall P., Liney G., Dosimetric optimization and commissioning of a high field inline MRI-linac, *Frontiers in Oncology*, 2020, **10**:136. [Crossref], [Google Scholar], [Publisher]

[11]. Patil D.B., Zope M.K., Beam commissioning data and quality assurance test for linear accelerator. *Journal of Indira Gandhi Institute Of Medical Sciences*, 2015, **40**:136 [Google Scholar], [Publisher]

[12]. Soto-Bernal T.G., Baltazar-Raigosa A., Medina-Castro D., Vega-Carrillo H.R., Neutron production in the interaction of 12 and 18 MeV electrons with a scattering foil inside a simple LINAC head, *Applied Radiation and Isotopes*, 2018, **139**:46 [Crossref], [Google Scholar], [Publisher]

[13]. Mesbahi A., Development a simple point source model for Elekta SL-25 linear accelerator using MCNP4C Monte Carlo code, *International Journal of Radiation Research*, 2006, **4**:7 [Google Scholar], [Publisher]

[14]. Khan F.M., Gibbons J.P., *Khan's the physics of radiation therapy*, Lippincott Williams & Wilkins, 2014 [Google Scholar], [Publisher]

[15]. Ramasamy V., Suresh G., Meenakshisundaram V., Gajendran V., Evaluation of natural radionuclide content in river sediments and excess lifetime cancer risk due to gamma radioactivity, *Research Journal of Environmental and Earth Sciences,* 2009, **1**:6 [Google Scholar], [Publisher]

[16]. Taskin H., Karavus M., Ay P., Topuzoglu A., Hidiroglu S., Karahan G., Radionuclide concentrations in soil and lifetime cancer risk due to gamma radioactivity in Kirklareli, Turkey, *Journal of environmental radioactivity*, 2009, **100**:49 [Crossref], [Google Scholar], [Publisher]

[17].Qureshi A.A., Tariq S., Din K.U., Manzoor S., Calligaris C., Waheed A., Evaluation of excessive lifetime cancer risk due to natural radioactivity in the rivers sediments of Northern Pakistan, *Journal of Radiation Research and Applied Sciences,*, 2014, **7**:438 [Crossref], [Google Scholar], [Publisher]

[18].Al Mashud M.A., Tariquzzaman M., Alam M.J., Zakaria G., Photon beam commissioning of an Elekta Synergy linear accelerator, *Polish Journal of Medical Physics and Engineering*, 2017, **23**:115 [Crossref], [Google Scholar], [Publisher]

**HOW TO CITE THIS ARTICLE**
Neda Zarei, Mohammad Reza Rezaie, Ali Jomehzadeh. Radiation Hazards Investigation of Photon Scattering by Elekta 6 MeV Linac during Liver Cancer Treatment. *Chem. Methodol.*, 2022, 6(8) 582-590
https://doi.org/10.22034/CHEMM.2022.338957.1493
URL: http://www.chemmethod.com/article_150334.html